HHS Public Access

Author manuscript

Cell Rep. Author manuscript; available in PMC 2018 May 23.

Published in final edited form as:

Cell Rep. 2018 April 10; 23(2): 499–511. doi:10.1016/j.celrep.2018.03.069.

How Biophysical Forces Regulate Human B Cell Lymphomas

F. Apoorva[1], **Alexander M. Loiben**[2], **Shivem B. Shah**[2], **Alberto Purwada**[2], **Lorena Fontan**[3], **Rebecca Goldstein**[3], **Brian J. Kirby**[1,3], **Ari M. Melnick**[3], **Benjamin D. Cosgrove**[2], and **Ankur Singh**[1,2,4,5]

[1]Sibley School of Mechanical and Aerospace Engineering, Cornell University, Ithaca, NY 14853, USA

[2]Nancy E. and Peter C. Meinig School of Biomedical Engineering, Cornell University, Ithaca, NY 14853, USA

[3]Division of Hematology/Oncology, Department of Medicine, Weill Cornell Medical College, New York, NY 10021, USA

[4]Englander Institute for Precision Medicine, Weill Cornell Medical College, New York, NY 10021, USA

Summary

The role of microenvironment-mediated biophysical forces in human lymphomas remains elusive. Diffuse large B cell lymphomas (DLBCLs) are heterogeneous tumors, which originate from highly proliferative germinal center B cells. These tumors, their associated neo-vessels, and lymphatics presumably expose cells to particular fluid flow and survival signals. Here, we show that fluid flow enhances proliferation and modulates response of DLBCLs to specific therapeutic agents. Fluid flow upregulates surface expression of B cell receptors (BCRs) and integrin receptors in subsets of ABC-DLBCLs with either CD79A/B mutations or WT BCRs, similar to what is observed with xenografted human tumors in mice. Fluid flow differentially upregulates signaling targets, such as SYK and p70S6K, in ABC-DLBCLs.By selective knockdown of *CD79B* and inhibition of signaling targets, we provide mechanistic insights into how fluid flow mechanomodulates BCRs and integrins in ABC-DLBCLs. These findings redefine microenvironment factors that regulate lymphoma-drug interactions and will be critical for testing targeted therapies.

Graphical abstract

Correspondence to: Ankur Singh.

[5]Lead Contact

Supplemental Information: Supplemental Information includes Supplemental Experimental Procedures, seven figures, and three videos and can be found with this article online at https://doi.org/10.1016/j.celrep.2018.03.069.

Author Contributions: F.A. conducted all experiments, collected data, performed data analysis, and wrote the manuscript with A.S. A.M.L. and B.D.C. performed phosphorylation analysis. S.B.S. and A.P. assisted with experiments. B.J.K. advised on computational simulations. L.F., R.G., and A.M.M. provided reagents. A.S. developed the concept and with F.A. contributed to the planning and design of the project.

Declaration of Interests: The authors declare no competing interests.

Apoorva et al. report a lymphoma micro-reactor to understand biophysical factors that regulate lymphoma growth and their therapeutic responses. They describe the role of fluid forces, from lymphatics and neo-vessels, in mechanomodulation of integrin and B cell receptor signaling. These insights shed light on the heterogeneous nature of lymphomas and may allow faster translation of therapeutics.

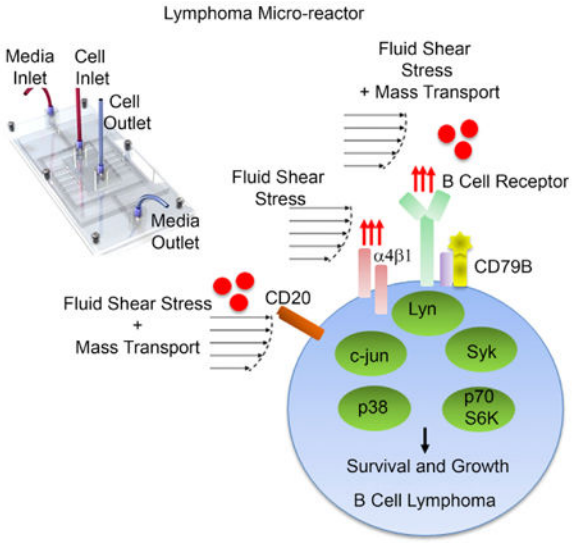

Introduction

Diffuse large B cell lymphomas (DLBCLs) are lymphoproliferative tumors that arise from proliferative immune cells in lymphoid tissues. Gene expression profiling has enabled DLBCLs to be sub-classified into germinal center B cell (GCB) DLBCL and activated B cell (ABC) DLBCL subtypes (Alizadeh et al., 2000; Davis et al., 2001, 2010; Fontán and Melnick, 2013; Fontan et al., 2012). The current therapy involves a chemo-immunotherapy regimen containing CHOP (cyclophosphamide, hydroxyldaunomycin [doxorubicin], oncovin [vincristine], and prednisone) with rituximab (a chimeric anti-CD20 IgG1 monoclonal antibody). However, a significant percentage of DLBCL patients are not cured by this treatment (Friedberg, 2011). ABC-DLBCL is the most chemoresistant DLBCL subtype with a 5-year overall survival as low as 45% versus 80% for GCB DLBCL (Lenz et al., 2008b; Roschewski et al., 2014). Understanding factors that promote resistance to drug therapy and identifying new therapeutic targets are important to improve clinical outcome of DLBCL patients.

Targeting hallmark pathways of ABC-DLBCL, such as those downstream of the chronically activated B cell receptor (BCR) signaling (Burger and Wiestner, 2018; Davis et al., 2010; Fontan et al., 2012; Wilson et al., 2015), has the potential to impact a broad cross-section of ABC-DLBCL patients (Brower, 2015; Wilson et al., 2015). Importantly, even when chronically activated by somatic mutations, the BCR pathway still needs signals from the microenvironment to drive cell survival, and yet extracellular factors that regulate BCR signaling remain less understood. The BCR is a transmembrane protein complex composed of heavy-chain and light-chain immunoglobulins (Igs), CD79A/Igα and CD79B/Igβ;

(Küppers, 2005). ABC-DLBCLs commonly manifest somatic mutation of components in the BCR pathway, such as CD79A/B (~20% of ABC-DLBCLs) (Davis et al., 2010), CARD11 (~10%) (Lenz et al., 2008a), and several others. Proposed therapeutic strategies for ABC-DLBCL target proteins signaling downstream of the BCR pathway, including kinase inhibitors targeting spleen tyrosine kinase (SYK), and Bruton's tyrosine kinase (BTK), among others (Burger and Wiestner, 2018; Fontán and Melnick, 2013). However, the pattern of response to BCR-targeted therapies varies according to mutations present in a given ABC-DLBCL. For example, a SYK short hairpin RNA (shRNA) suppresses the growth of ABC-DLBCL cell line, HBL-1 (Davis et al., 2010), which expresses a CD79B mutation in the IgM BCR. In contrast, SYK shRNA is less effective in the ABC-DLBCL cell line, OCI-LY10, with a CD79A mutation. This underscores the need for better understanding the regulators of BCR signaling in heterogeneous subclasses of ABC-DLBCLs, under growth conditions that mimic tumor microenvironment.

A major impediment in the field is that, unlike other tumors, the importance of the physical nature of the lymphoma microenvironment has not been studied in detail (Scott and Gascoyne, 2014). We have recently shown that the cross talk between lymphoid tissue's extracellular matrix, stiffness, and integrins on lymphoma cells are critical for tumor cell survival and signaling, both *in vitro* and *in vivo* (Apoorva et al., 2017; Cayrol et al., 2015; Tian et al., 2015). Once DLBCL cells seed a lymphoid tissue, malignant B cells proliferate steadily, causing massive distortion, enlargement, and vascularization of these tumor-seeded tissues as shown by us (Ruan et al., 2013) and others (Ruan et al., 2009). The increased vascularization and lymphatic flow presumably expose the lymphoma cells to fluid flow, i.e., fluid shear stress (tangential forces on cell surface) and nutrient mass transport, which supports their survival, proliferation, and response to drugs. Here, we have endeavored to determine how fluid forces regulate human lymphomas. Because the fluid shear stress values in enlarged, vascularized lymphoma tissues are also unknown, the current study focuses on uncovering the biological impact of biophysical forces at the peak fluid shear stress of 0.8–1.3 dyn/cm^2, reported earlier to be applicable in the subcapsular sinus lumen of lymphoid tissues (Jafarnejad et al., 2015). Conventional tissue culture plates, which do not induce shear stress and large bioreactors (shear stress of 6–12 dyn/cm^2) are not suitable to study the effect low fluid shear stresses in the range of 0.8–1.3 dyn/cm^2. Here, using an *ex vivo* lymphoma micro-reactor platform and inhibiting various key signaling proteins and knocking down a CD79 complex, we demonstrate, for the first time to our knowledge, that fluid shear stress alone or in combination with nutrient mass transport can act as an important biophysical stimulus on DLBCLs by influencing the BCR and integrin signaling, with consequences on cell proliferation, differentially dependent on heterogeneous DLBCL subclasses.

Results and Discussion

Ex Vivo Lymphoma Micro-Reactor with High-Resistance Channels

Our primary goal was to characterize how DLBCLs respond to fluid forces reported earlier in the subcapsular sinus lumen of lymphoid tissues. Therefore, we designed our micro-reactors to achieve a fluid shear stress of ~0.3–1.3 dyn/cm^2 (Figure 1A). Our secondary goal

was to maintain the pressure difference in the micro-reactor close to the physiological pressure difference of 1 mm Hg (or 133 Pa), previously reported between paracortex and afferent vessels (Jafarnejad et al., 2015). In addition, our goal was to ensure that fluid flow was uniformly distributed such that almost all of the cells in the micro-reactor were exposed to the same biophysical forces. An addition micro-reactor design criterion was to maintain DLBCL cells in 50% conditioned media through media recirculation (Tian et al., 2015).

To achieve our goal, we considered four micro-reactor designs (Figures 1B and S1–S3) and computationally modeled them to compare across above-mentioned critera. Engineering details and analysis of the computational results are included in Supplemental Experimental Procedures, Figures S1–S3, and Video S1. Of these four micro-reactors, two of the micro-reactors were chosen from previous reports where they showed utility in studying adherent cell types and hematopoietic lineages (Lecault et al., 2011; Yu et al., 2014). Our own two micro-reactors were a modification of recently described work (Nakao et al., 2011). These were designed to include a cell culture chamber that was connected to media chamber by 5-μm-wide high-resistance narrow channels, which dramatically reduced media flow velocity into the cell chamber (Figures 1B and 1C). One of our micro-reactors (called side flow) had media flow channel perpendicular to the high-resistance channel (Figures 1C and 1D), and the other micro-reactor (called cross flow) had media flow chamber aligned with the high-resistance channel (Figure S3). Based on computational analysis, we determined that the side-flow micro-reactors (Figure 1B) resulted in uniformly distributed flow patterns and shear stress (0.3–1.3 dyn/cm^2) with approximately 100% of the cell culture area exposed to a uniform fluid flow (Figure 1E). Importantly, the pressure difference across the side-flow micro-reactor was 100 Pa, which is very close to the physiological value of 1 mm Hg (or 133 Pa) (Jafarnejad et al., 2015). These two computational outputs benchmarked the superiority of our side-flow micro-reactor against alternative micro-reactor platforms tested in this study, where only 25%–66% area of the micro-reactor was exposed to uniform shear forces and the pressure difference was markedly below 1 mmHg (2–20 Pa; Figures 1E and S1E).

In the side-flow micro-reactors, cells were introduced into the central chamber using the “Cell Inlet” port (Figure 1B). The media was flown through the “Media Inlet” port and perfused into the central chamber as indicated by purple arrows in Figure 1B. The media was recirculated and diluted by connecting the “Media Inlet” and “Media Outlet” ports by means of a rotary pump (Figure 1C). The central cell culture chamber was connected to the circulating media channel (width, 20 mm) through high-resistance perfusion channels (width, 5 μm), which prevented the 8- to 10-μm cells from leaving the central cell chamber (Figure 1D). Dimensions of the central chamber were length 3 cm, height 100 mm, and width 0.6 cm. To prevent the top of cell culture chamber from collapsing, we included 40-μm-wide polydimethylsiloxane (PDMS) micro-pillars, separated by 800-μm distance within the central chamber of the micro-reactor (Figures 1C and 1D), which did not significantly affect the flow rate. Since DLBCLs are loosely adherent cells and conventionally cultured in tissue culture plates without any substrates, the micro-reactors were not pre-coated with any extracellular matrices. However, these cells can still adhere to serum proteins, such as fibronectin (Blonska et al., 2015), using integrin receptors. When DLBCL cells were cultured in these micro-reactors (without substrates) over 24 hr, lymphoma cells were

uniformly distributed throughout the micro-reactor and did not accumulate against the micro-reactor wall (Figure 1F). The cells in the micro-reactor showed excellent viability, as qualitatively determined using a live-dead assay (Figure 1F).

Fluid Flow Enhances Proliferation of Human DLBCL Cells and Regulates Drug-Induced Apoptosis in Lymphoma Cells

We hypothesized that in contrast to static growth conditions, fluid flow, either as shear stress alone or in combination with mass transport, will modulate proliferation of lymphoma cells through mechanical stimulation of surface receptors such as integrins. Our secondary hypothesis was that fluid flow-mediated changes in integrin stimulation will modulate BCR through outside-in cross talk. We first examined the role of fluid flow on the growth of BCR-dependent ABC-DLBCL cell lines (Figure 1G) with CD79A mutations (OCI-LY10) and CD79B mutations (HBL-1). We exposed OCI-LY10 and HBL-1 to a fluid flow (i.e., shear stress of ~1.3 dyn/cm^2). We observed significantly higher proliferation that started as early as day 3 in flow conditions compared to static cultures and continued to grow with time (Figure 1H).

Although DLBCL cell lines are not traditionally cultured with immune or stromal supports, researchers have explored the use of follicular dendritic cells in lymphoma cultures as immune-stromal support (Yoon et al., 2010). Therefore, we incorporated human tonsil-derived follicular dendritic cells (Tian et al., 2015; Yoon et al., 2010) into these cultures (Figure 1I). A 48-hr cell proliferation analysis confirmed that even in the presence of follicular dendritic cells, both OCI-LY10 and HBL-1 proliferated more under flow conditions than static conditions (Figure 1J), suggesting that micro-reactors are suitable for mono- and co-cultures of DLBCLs.

We next determined whether fluid flow changes the abundance of cytokines secreted by OCI-LY10 and HBL-1 cells in the media, which could have autocrine and paracrine effects. As indicated in Figure 1K, we observed a significant increase in tumor necrosis factor α (TNFα) and granulocyte-macrophage colony-stimulating factor (GM-CSF) in media from OCI-LY10 cells grown under flow conditions for 72 hr. In contrast, there was no significant change in aforementioned proteins in media from HBL-1 cells grown under flow conditions. There was modest or no difference in the remaining tested cytokines (interferon γ [IFN-γ], interleukin-1A [IL-1A], IL-17A, IL-1B, IL-4, IL-6, IL-8, and IL-12) (Figure S4). Several of these cytokines play an important and widespread role in cancer (Hodge et al., 2005; Kawano et al., 1988; Lam et al., 2008; Ngo et al., 2011; Yang et al., 2012; Yee et al., 1989).

Since DLBCLs proliferate better under flow conditions, we hypothesized that the healthier status of cells under flow conditions will reduce the apoptosis of ABC-DLBCLs when exposed to anti-lymphoma drugs. We first determined the uptake of the drug doxorubicin by DLBCLs under static and flow conditions using flow cytometry (doxorubicin is fluorescent; Frank et al., 2005). These experiments were performed by culturing DLBCLs in micro-reactors for 72 hr, followed by exposure to the drug. We did not observe significant differences in uptake of the drug over 24–36 hr (Figure 2A). Both HBL-1 and OCI-LY10 cells exhibited a significant decrease in apoptosis (Annexin-V+) when exposed to doxorubicin under flow conditions (Figures 2B–2D). Finally, we tested whether the reduced

apoptosis could be extended to other classes of anti-cancer therapeutics and evaluated the response to a histone deacetylase inhibitor (HDACi) (Panobinostat) under flow conditions. As illustrated in Figure 2E, a similar pattern of reduced apoptosis was observed under flow conditions compared to static conditions. Collectively, these results suggest that drug-induced DLBCL apoptosis is affected by the presence of fluid flow.

Fluid Flow Upregulates the Surface Expression of BCRs and Integrin Receptors in ABC-DLBCL, Similar to Xenografted Human Tumors in Mice

The BCR is vital for the growth of ABC-DLBCL through downstream pathways and abrogation of BCR signaling results in proliferation arrest of ABC-DLBCL (Davis et al., 2010; Fontan et al., 2012). Hence targeting of BCR signaling pathways has emerged as a promising therapeutic approach for these tumors (Brower, 2015; Fontan et al., 2012; Goldstein et al., 2015; Wilson et al., 2015). To determine whether flow conditions affect the level of expression of the BCR, which could affect its signaling, we measured the levels of IgM BCR, by flow cytometry. As indicated in Figures 3A, top, and 3B, in HBL-1 ABC-DLBCLs (CD79B mutation), cell surface expression of IgM was significantly increased by 3.8-fold under flow conditions. By contrast, in OCI-LY10 ABC-DLBCLs (CD79A mutation), there was no change under flow conditions. Notably, OCI-LY3 ABC-DLBCL cells, which have WT CD79A/B, also exhibited significantly increased IgM expression under flow conditions. However, no differences were observed in the GCB-DLBCL cell line OCI-LY1. Collectively, these findings suggest that true levels of expression of the BCR are under-appreciated in 2D static cultures and the BCR expression is differentially upregulated among subsets of ABC-DLBCLs.

Although the majority of B cell lymphomas express surface CD20 receptor, only 76% of patients respond to CHOP plus rituximab (Coiffier et al., 2002) and 50% to rituximab alone (McLaughlin et al., 1998; Wojciechowski et al., 2005). The differences in response have been attributed to decreased CD20 expression observed in some patients treated with rituximab (Wojciechowski et al., 2005). Therefore, understanding mechanisms that regulate CD20 expression is important. We determined the effect of fluid shear stress on CD20 expression by exposing the cells to either static or flow conditions. As indicated in Figure 3C, fluid flow induced 3.5-fold higher upregulation of CD20 on the surface of OCI-LY10 cells ($p < 0.05$). In contrast, we observed only 1.3-fold upregulation of CD20 in HBL-1 cells.

Integrins have been shown to play important roles in transmitting mechanical stimuli received from fluid shear stress into intracellular signals in a wide variety of cells (Lee et al., 2010; Tzima et al., 2001). In lymphoid cells, integrins can function as pro-survival signals (Blonska et al., 2015; Cayrol et al., 2015), and upregulation of $\alpha 4\beta 1$ integrins in DLBCLs provides a protective pro-survival signal (Tian et al., 2015; Tjin et al., 2006). We, therefore, determined the role of fluid shear stress on the expression of $\alpha 4\beta 1$ integrins on ABC-DLBCL cells. Flow induced a significant 1.7-fold higher expression of $\alpha 4$ subunits in OCI-LY10 and a 4.3-fold increase in HBL-1 (Figures 3A, bottom, and 3D). No differences were observed in OCI-LY3 and OCI-LY1 cells. HBL-1 cells also exhibited a significant 1.3-to 1.5-fold increase in the $\beta 1$ integrin subunit under flow conditions ($p < 0.05$) (Figures 3E and

S5A). These findings suggest that the expression levels of integrin mechanoreceptors on ABC-DLBCL cells are dependent on fluid forces.

To determine whether changes in BCR and integrin expression were observed *in vivo*, we performed a direct comparison of HBL-1 and OCI-LY10 cell lines to their xenografted tumors in immunocompromised NSG (NOD.Cg-Prkdcscid Il2rgtm1Wjl/SzJ) mice, a model of choice for cancer xenograft modeling. Xenografts were harvested when tumors grew, and BCR, integrin α4, and integrin β1 levels were evaluated to compare with their levels on cells before implantation (representing static conditions). As indicated in Figure 3F, tumors developed in NSG mice implanted with OCI-LY10 xenografts, often well vascularized. Flow-cytometric analysis showed higher mean fluorescence intensity in integrin α4 signal in xenografted cells (Figure 3F, bottom). Quantitative analysis of the surface expression level of IgM (as a measure of the BCR), integrin α4, and integrin β1 on HBL-1 xenografts under static (*in vitro* conditions) versus *in vivo* conditions show a similar pattern of differential expression as was observed in our micro-reactors (Figures 3F, right, and 3G). These results clearly demonstrate that lymphoma micro-reactors are more similar to tumors *in vivo*, therefore confirming the power and importance of a microfluidic-based model system.

We were intrigued by the question of what these integrin receptors bind to in a tissue culture system that is not pre-coated with an extracellular matrix. Although lymphomas are loosely adherent cells, in our experiments we did not see these cells moving under flow conditions. This led us to hypothesize that there was weak but significant adhesion between DLBCLs and the underlying glass substrate in the micro-reactors, likely due to the serum proteins deposited from the media. Since β1 is a common integrin subunit involved in dimerization with multiple α subunits, including α4 and α5, we determined whether β1 integrin was involved in adhesion of DLBCL cells to the underlying surface. When integrin β1 was blocked using a monoclonal anti-β1 antibody, HBL-1 ABC-DLBCL cells accumulated at the edges and a few high-resistance channels of the micro-reactor through which media is supposed to exit the cell culture chamber (Figure 3H; Videos S2 and S3).In contrast, in the absence of blocking anti-β1 integrin antibody, the cells remained in their initial position, suggesting that β1 integrin was a surface receptor involved in adhesion to the floor of the micro-reactors. Unlike HBL-1, blocking β1 integrin did not markedly affect the adhesion of OCI-LY10 under flow conditions despite the fact that both HBL-1 and OCI-LY10 express similar levels of integrin β1 (Figures S5B and S5C). Finally, we also tested whether α5 integrin was expressed by these cells and observed a very modest increase in HBL-1 cells grown in flow conditions, but not in OCI-LY3 and OCI-LY10 (Figure 3I), suggesting α5 integrin may not play an important role in our observations.

We also determined whether the pattern of increase or decrease in these surface receptors under fluid flow was maintained under three-dimensional (3D) extracellular matrix rich conditions, which involve different relative tangent and normal shear stresses. We encapsulated ABC-DLBLCs in Matrigel matrix inside the micro-reactors and exposed them to the same shear stress (1.3 dyn/cm^2) as in the 2D micro-reactors. The change in BCR and integrin α4 followed similar patterns as in conditions without a matrix (Figure S5D). However, we observed consistent upregulation of β1 subunit, which could be attributed to the engagement of β1 integrins by Matrigel, causing their upregulation (Poincloux et al.,

2011). Although we chose Matrigel for this study because of its extensive use by others in the cancer field, we have previously shown that ABC-DLBCL subtypes have a heterogeneous need for integrin subtypes for survival and Matrigel may not be the ideal matrix (Singh et al., 2018; Tian et al., 2015). Therefore, future studies will focus on understanding the role of fluid flow and ligands specific to the integrin receptors found on each DLBCL subtype.

Fluid Flow Differentially Regulates Phosphorylation of Complementary Signaling Pathways in ABC-DLBCLs

To understand the mechanism of signaling through the integrin and BCR pathways induced by fluid flow, we exposed ABC- and GCB-DLBCLs to fluid flow (1.3 dyn/cm^2) and examined phosphoprotein levels of various downstream proteins using multiplexed bead-based Luminex assays (Cosgrove et al., 2010). A GCB-DLBCL cell line, OCI-LY1, was used as a negative control. Since we observed that surface expression of BCR is differentially modulated in ABC-DLBCL cells under flow conditions, we determined the phosphorylation of immediate downstream molecules LYN (p-Lyn) and SYK (p-SYK), which are critical for activation of the BCR. We found that p-LYN and p-SYK exhibited >2-fold increase in HBL-1 due to fluid flow exposure, whereas, in OCI-LY10, there was no change due to fluid flow (Figures 4A and 4B). p-LYN was also increased in OCI-LY3 cells; however, no significant increase in p-SYK was observed. We further observed no change in p-LYN and p-SYKinOCI-OCI-LY1 cells under flow conditions. Upregulation of p-LYN and p-SYK with HBL-1 (CD79B mutant) but not in OCI-LY10 (CD79A mutant) is in agreement with our observations in Figure 3 that there is significant upregulation of the BCR in HBL-1, and not in OCI-LY10. Our observations are further aligned with the finding by Staudt and colleagues (Davis et al., 2010) that shRNA targeting SYK suppresses the growth of ABC-DLBCL line HBL-1 but not OCI-LY10, OCI-LY3, or GCB-DLBCL lines. Typically, BCR activation can trigger downstream AKT signal, which activates mechanistic target of rapamycin (mTOR) by inhibiting the tuberous sclerosis complex, leading to p70S6K activation. We observed elevated levels of p-AKT in these cells and p-p70SK expression level was increased by a significant >3-fold in HBL-1 when exposed to fluid flow, where as OCI-LY10 showed a marginal decrease or no change with fluid flow (Figures 4C and S6).

We next explored the impact of fluid flow on the MAPK signaling pathway (Dai et al., 2009; Nguyen et al., 2010), which is also linked to the BCR receptor pathway (Figures 4D–4F). The phosphorylation of p38 and the downstream target cJUN was increased >3-fold in HBL-1 and 2-fold in OCI-LY3, when exposed to the fluid flow. In contrast, OCI-LY10 and OCI-LY1 showed a marginal decrease or no change with fluid flow. While OCI-LY3 manifested a small but significant increase in p-ERK levels under flow conditions, no such increase was observed in OCI-LY10 and HBL-1 cells.

Understanding the Contributions of Fluid Shear Stress and Mass Transport in ABC-DLBCL Surface Receptor Expression

The differences seen in the expression of the surface receptors can be attributed to the effect of fluid shear stress (i.e., more forces on cell receptors from the flow), or increased mass transport (i.e., faster removal of secreted factors and metabolic products because the flow

carries them away), or both. We created matched experiments with culture solutions with different transport properties to establish that shear stress at the cell surface plays a prominent role in generating the differences seen in BCR, integrin, and CD20 expression. We added dextran to the culture solution to increase the solution viscosity and thus increase the tangential stress on cells in flow (Figures 5A–5E). Adding dextran reduces the rate at which species diffuse toward or away from the cell (Li et al., 2009). The addition of 1% dextran increased the viscosity by ten times (Figure S7A) and is expected to have decreased solute molecular diffusivity by a similar amount. We then performed the following comparisons: (1) compared static culture with and without dextran, where the addition of dextran reduced solute molecular diffusivity and is expected to reduce transport of secreted factors and metabolic products, and (2) compared flow culture with and without dextran, in which we increased the viscosity of flow media and reduced flow by ten times to maintain the same tangential shear stress (1.3 dyn/cm^2). For the flow culture comparison, the flow with dextran had lower diffusion of species than that without dextran because the dextran reduced solute diffusivity. Furthermore, the flow with dextran had lower convection of species than that without dextran because for the same tangential shear stress a lower velocity flow was used.

Under these defined conditions, we found that there was no effect of flow versus flow (viscous) on α4 integrin mechanoreceptor expression in HBL-1 cells (Figure 5A). This suggests that the increase in α4 integrin in HBL-1 cells is primarily due to fluid shear stress and not diffusive or convective-diffusive mass transport. In contrast, OCI-LY10 cells showed a significant decrease in α4 integrin expression under viscous flow conditions compared to regular flow conditions. Because fold-change values in flow (viscous) conditions were still higher than under static conditions, we concluded that the effect in OCI-LY10 is a combined contribution from mass transport and fluid shear stress. We did not see differences in α4 integrin expression in static versus static (viscous) for OCI-LY3 or HBL-1 (Figure 5D).

The cell surface expression of the remaining markers, CD20, β1 integrin, and BCR (Figures 5A–5D), showed a significant decrease in surface expression in OCI-LY10 and HBL-1 cells when cultured under flow (viscous) conditions compared to flow conditions. Because expression under flow (viscous) values were still higher than static conditions, we concluded that the effect in HBL-1 and OCI-LY10 were a combinatorial effect of mass transport and fluid shear stress for these receptors. The only exception here is the expression of integrin β1 in OCI-LY10, which showed an increase in surface expression under viscous conditions, the reasons for which are not yet clear and will require further investigation. We further compared static (viscous) versus static conditions and determined that there was no significant difference in IgM/BCR and b1 integrin expression levels in HBL-1 (Figure 5E).

Mechanistic Model of Fluid Flow-Mediated Mechanomodulation of ABC-DLBCLs

Based on our findings in previous sections, we propose a mechanomodulation model in HBL-1 ABC-DLBCLs. Here, fluid flow upregulates the cell surface expression of IgM, integrin α4, and integrin β1, which in turn increases phosphorylation of LYN, SYK, p38, c-JUN, and p70S6K, and affects cell proliferation (Figure 6A). In contrast, fluid flow does not upregulate IgM and integrin signaling in OCI-LY10 and other complementary mechanisms

may be responsible for its proliferation. To prove our hypothesis, we blocked integrin receptors by using an anti-α4β1 antibody over 48 hr and observed statistically significant ~50% decrease in proliferation of HBL-1 but no decrease in OCI-LY10 cells (Figure 6B). These findings indeed support the hypothesis that fluid flow mechanomodulates integrin receptors to control HBL-1 proliferation.

To further understand the role of IgM BCR and the interplay of signaling molecules that are upregulated in HBL-1 ABC-DLBCLs, we first inhibited SYK by using two complementary SYK inhibitors, R406 or PRT062607. The dose of R406 and PRT062607 was chosen at the maximum inhibitory dose, which is capable of inhibiting the activity of signaling target but remains non-toxic (cell survival, 94% ± 4%; Figure S7B). As indicated in Figure 6C, inhibition of SYK (R406, 200 nM) prevented an increase in HBL-1 proliferation under flow conditions, suggesting that SYK signaling regulates cell proliferation. Inhibition of SYK did not reduce the integrin β1 expression levels under flow conditions (Figure 6D), suggesting that the limiting of proliferation was attributable to the blocking of SYK signaling, independent of any effect in modulating integrin expression levels. We further verified our results by using PRT062607 (Geng et al., 2015) at 5 nM dose. The anti-SYK activity of PRT062607 is at least 80-fold greater than for other kinases (Spurgeon et al., 2013). As shown in Figure 6E, cell proliferation and expression of integrin α4 and β1 was similar between R406 and PRT062607. We next inhibited p70S6K using an mTOR inhibitor at 0.5 nM dose (maximum inhibitory dose while still maintaining ~95% viability). As indicated in Figure 6F, inhibition of mTOR prevented an increase in HBL-1 proliferation under flow conditions, suggesting that p70S6K signaling also regulates cell proliferation. The mTOR inhibitor did not reduce the IgM expression under flow conditions (Figures 6G and S7C), suggesting that the limited proliferation was attributable to the blocking of downstream p70S6K signaling and not a reduction in IgM BCR expression.

The CD79B Complex in BCR Cross Talks with Integrins under Fluid Flow Conditions to Mechanomodulate Human DLBCLs

Finally, we tested whether the CD79B protein in HBL-1 is a target of fluid flow-based mechanomodulation and whether it modulates integrin-BCR cross talk. To study this, we used doxycycline-inducible shRNAs against *CD79B* (or Luciferase as control), which were validated using western blot analysis (Figures 7A and S7D). When exposed to doxycycline to induce the shRNA, the cells expressed GFP (Figures 7B and S7E), and the induced shRNA reduced expression of CD79B. Under flow conditions, doxycycline-inducible shRNA knockdown of CD79B in HBL-1 cells led to significantly decreased proliferation of total cells as well as GFP^+ cells compared to HBL-1 cells transduced with the control shLuc (Figure 7C). Furthermore, under flow conditions, knockdown of the CD79B significantly reduced integrin β1 expression to the levels of static conditions with CD79B knockdown (Figure 7D). In contrast, induction of shRNA against luciferase in HBL-1 cells as a control did not reduce integrin β1 expression. In the same studies, under flow conditions, knockdown of the CD79B did not reduce upstream IgM/BCR expression levels (Figure 7E). Last, we observed a significant reduction of pSYK and pLYN expression in as well as GFP^+ cells treated with shRNA against CD79B, but not with shRNA against Luciferase (Figures 7F and 7G). The decrease in pSYK and pLYN correlates with the decrease in cell number

when CD79B is knocked out, and confirms that the increase in tumor growth under fluid flow conditions is partially mediated by downstream activation of SYK and LYN, as proposed in the model in Figure 6. Knocking down CD79B in HBL-1 cells under static conditions did not affect pSYK levels (Figure S7F). These new findings provide mechanistic insight into the cross talk of fluid flow, integrin β1, and CD79B, and may explain how heterogeneous subtypes of ABC-DLBCLs are differentially influenced by fluid flow.

Conclusions

This study highlights how complex biophysical forces in lymphomas differentially regulate heterogeneous B cell lymphoma subtypes and the expression levels of surface receptors, as well as downstream signaling proteins, which otherwise remain comparable under static culture conditions. Our current findings underscore the need for a lymphoma micro-reactor platform that is more biologically similar to the situation *in vivo* than a simple static 2D culture, to better understand the biology and predict the response of lymphomas to drugs. While it has been shown that CD79A/B mutations do not enhance BCR clustering, nor are they better at inducing nuclear factor κB (NF-κB) activity than their wild-type counterparts, our studies demonstrate that fluid flow has a differential effect on ABC-DLBCL subsets. Future studies will explore whether the differences observed could also be attributed to CD79A/B mutations themselves or other downstream mutations, such as those in CARD11. Future investigations will also determine the effect of knocking down/disrupting multiple pathways and understanding the role of fluid flow in new classes of therapeutic inhibitors (such as those targeting BCR signaling pathway). In the current study, we used fluid shear stresses reported for subcapsular sinuses in lymphoid tissues; however, more detailed measurements of fluid flow and associated stresses in lymphoma tissues need to be performed in a tumor-specific manner, followed by integration into the micro-reactors to model the effect outside of the body. Understanding the fluid flow-mediated effect on lymphomas could provide mechanistic insight into why some DLBCLs are sensitive to treatment while others are refractory and, importantly, allow a faster and more rational translation of targeted therapeutic regimens.

Experimental Procedures

Cell Culture in Lymphoma Micro-Reactors

In all studies, we loaded 100,000 DLBCL cells per micro-reactor. In studies that involved human tonsil-derived follicular dendritic cells, co-cultures were seeded at 1:1 ratio, with total cell number being 200,000 per micro-reactor. Static conditions were chosen as standard 2D non-treated tissue culture plates, which are routinely used in lymphoma research. Remaining details of cell lines, flow cytometry, and phosphoprotein levels are included in Supplemental Experimental Procedures.

Human Cell Line Xenografts in NSG Mice

NSG mice (6–8 weeks) were implanted with OCI-LY10 and HBL-1 xenografts. Bilateral tumor grafts (10^6 cell/injection) were implanted into the subcutaneous pockets (retronucal and caudal regions) using a syringe with Matrigel. The cut edges were sealed with a suture of fibrin glue. Tumor development was monitored, and mice were sacrificed at a pre-

determined time point. All studies were performed in compliance with the Institutional Animal Care and Use Committee (IACUC) approval at Cornell University.

Inducible shRNA-Mediated CD79B Knockdown

shRNAs were delivered by lentivirus infection, which were produced by transfection of 293T cells with the LT3GEPIR vector (Fellmann et al., 2013). Infected HBL1 cells were selected by puromycin treatment (1 μg/mL). Doxycycline (1 μg/mL) was used to induce the expression of the indicated shRNAs along with GFP, which was used to monitor shRNA expression. Mature antisense sequences of shRNA used to knockdown CD79B and Luciferase were as follows: shCD79B#744, 5′-TTCAGCTGTGCCAAGGTGCTGA-3′, and shLuciferase, 5′-TTAATCAGAGACTTCAGGCGGT-3′, respectively. Negative control included cells not treated with doxycycline. The knockdown of CD79B was validated by western blot analysis. For micro-reactor experiments, after 48 hr of treatment with doxycycline, cells were exposed to flow or static conditions for 72 hr, and doxycycline concentration was maintained during the course of the experiment. The phospho-SYK (Tyr525/526) (C87C1; #2710) and phospho-LYN (Tyr507) (#2731) were purchased from Cell Signaling Technology. A donkey anti-rabbit IgG H&L (Alexa Fluor 647; Abcam; ab150075) secondary antibody against these primary antibodies was used for detecting expression levels of pSYK and pLYN.

Statistical Analysis

Statistical analysis was performed using a two-tailed unpaired t test or a one-way ANOVA with Tukey's post hoc test or a two-way ANOVA with Bonferroni's correction. Statistical analysis for each plot is described in the figure legend. Statistical analyses were performed using GraphPad Prism software and a p value of less than 0.05 was considered significant. All values are reported as mean ± SEM. Data presented in this manuscript are a triplicate experiment representative of at least three independent experiments, except the NSG mice study.

Supplementary Material

Refer to Web version on PubMed Central for supplementary material.

Acknowledgments

The authors acknowledge partial financial support from the National Institutes of Health (1R33CA212968-01 and 1R01AI132738-01A1 to A. S. and R00AG042491 to B.D.C.), Department of Defense Career Development Award (W81XWH-17-1-0215 to A.S.), and the National Science Foundation (CBET-1511914 to A.S. and B.J.K.). The authors acknowledge support from Graduate Assistantships in Areas of National Need from the U.S. Department of Education Grant P200A150273 to A.M.L. and S.B.S. This work was performed in part at Cornell NanoScale Facility (CNF), a National Nanotechnology Coordinated Infrastructure (NNCI) member supported by National Science Foundation Grant ECCS-1542081. The authors acknowledge Scott Butler, Rishi Puri, and Dr. Kristy Richards of Cornell's Progressive Assessment of Therapeutics (PATh) program for assisting with the xenograft models. We are thankful to Prof. Avery August (Cornell University) for providing feedback on the revised manuscript. Opinions, interpretations, conclusions, and recommendations are those of the authors and are not endorsed by the funding agencies.

References

Alizadeh AA, Eisen MB, Davis RE, Ma C, Lossos IS, Rosenwald A, Boldrick JC, Sabet H, Tran T, Yu X, et al. Distinct types of diffuse large B-cell lymphoma identified by gene expression profiling. Nature. 2000; 403:503–511. [PubMed: 10676951]

Apoorva FNU, Tian YF, Pierpont TM, Bassen DM, Cerchietti L, Butcher JT, Weiss RS, Singh A. Award Winner in the Young Investigator Category, 2017 Society for Biomaterials Annual Meeting and Exposition, Minneapolis, MN, April 05–08, 2017: Lymph node stiffness-mimicking hydrogels regulate human B-cell lymphoma growth and cell surface receptor expression in a molecular subtype-specific manner. J Biomed Mater Res A. 2017; 105:1833–1844. [PubMed: 28177577]

Blonska M, Zhu Y, Chuang HH, You MJ, Kunkalla K, Vega F, Lin X. Jun-regulated genes promote interaction of diffuse large B-cell lymphoma with the microenvironment. Blood. 2015; 125:981–991. [PubMed: 25533033]

Brower V. Ibrutinib promising in subtype of DLBCL. Lancet Oncol. 2015; 16:e428.

Burger JA, Wiestner A. Targeting B cell receptor signalling in cancer: preclinical and clinical advances. Nat Rev Cancer. 2018; 18:148–167. [PubMed: 29348577]

Cayrol F, Díaz Flaqué MC, Fernando T, Yang SN, Sterle HA, Bolontrade M, Amorós M, Isse B, Farías RN, Ahn H, et al. Integrin αvβ3 acting as membrane receptor for thyroid hormones mediates angiogenesis in malignant T cells. Blood. 2015; 125:841–851. [PubMed: 25488971]

Coiffier B, Lepage E, Briere J, Herbrecht R, Tilly H, Bouabdallah R, Morel P, Van Den Neste E, Salles G, Gaulard P, et al. CHOP chemotherapy plus rituximab compared with CHOP alone in elderly patients with diffuse large-B-cell lymphoma. N Engl J Med. 2002; 346:235–242. [PubMed: 11807147]

Cosgrove BD, Alexopoulos LG, Hang TC, Hendriks BS, Sorger PK, Griffith LG, Lauffenburger DA. Cytokine-associated drug toxicity in human hepatocytes is associated with signaling network dysregulation. Mol Biosyst. 2010; 6:1195–1206. [PubMed: 20361094]

Dai B, Zhao XF, Hagner P, Shapiro P, Mazan-Mamczarz K, Zhao S, Natkunam Y, Gartenhaus RB. Extracellular signal-regulated kinase positively regulates the oncogenic activity of MCT-1 in diffuse large B-cell lymphoma. Cancer Res. 2009; 69:7835–7843. [PubMed: 19789340]

Davis RE, Brown KD, Siebenlist U, Staudt LM. Constitutive nuclear factor kappaB activity is required for survival of activated B cell-like diffuse large B cell lymphoma cells. J Exp Med. 2001; 194:1861–1874. [PubMed: 11748286]

Davis RE, Ngo VN, Lenz G, Tolar P, Young RM, Romesser PB, Kohlhammer H, Lamy L, Zhao H, Yang Y, et al. Chronic active B-cell-receptor signalling in diffuse large B-cell lymphoma. Nature. 2010; 463:88–92. [PubMed: 20054396]

Fellmann C, Hoffmann T, Sridhar V, Hopfgartner B, Muhar M, Roth M, Lai DY, Barbosa IA, Kwon JS, Guan Y, et al. An optimized micro-RNA backbone for effective single-copy RNAi. Cell Rep. 2013; 5:1704–1713. [PubMed: 24332856]

Fontán L, Melnick A. Molecular pathways: targeting MALT1 para-caspase activity in lymphoma. Clin Cancer Res. 2013; 19:6662–6668. [PubMed: 24004675]

Fontan L, Yang C, Kabaleeswaran V, Volpon L, Osborne MJ, Beltran E, Garcia M, Cerchietti L, Shaknovich R, Yang SN, et al. MALT1 small molecule inhibitors specifically suppress ABC-DLBCL in vitro and in vivo. Cancer Cell. 2012; 22:812–824. [PubMed: 23238016]

Frank NY, Margaryan A, Huang Y, Schatton T, Waaga-Gasser AM, Gasser M, Sayegh MH, Sadee W, Frank MH. ABCB5-mediated doxorubicin transport and chemoresistance in human malignant melanoma. Cancer Res. 2005; 65:4320–4333. [PubMed: 15899824]

Friedberg JW. Relapsed/refractory diffuse large B-cell lymphoma. Hematology (Am Soc Hematol Educ Program). 2011; 2011:498–505. [PubMed: 22160081]

Geng H, Hurtz C, Lenz KB, Chen Z, Baumjohann D, Thompson S, Goloviznina NA, Chen WY, Huan J, LaTocha D, et al. Self-enforcing feedback activation between BCL6 and pre-B cell receptor signaling defines a distinct subtype of acute lymphoblastic leukemia. Cancer Cell. 2015; 27:409–425. [PubMed: 25759025]

Goldstein RL, Yang SN, Taldone T, Chang B, Gerecitano J, Elenitoba-Johnson K, Shaknovich R, Tam W, Leonard JP, Chiosis G, et al. Pharmacoproteomics identifies combinatorial therapy targets for diffuse large B cell lymphoma. J Clin Invest. 2015; 125:4559–4571. [PubMed: 26529251]

Hodge DR, Hurt EM, Farrar WL. The role of IL-6 and STAT3 in inflammation and cancer. Eur J Cancer. 2005; 41:2502–2512. [PubMed: 16199153]

Jafarnejad M, Woodruff MC, Zawieja DC, Carroll MC, Moore JE Jr. Modeling lymph flow and fluid exchange with blood vessels in lymph nodes. Lymphat Res Biol. 2015; 13:234–247. [PubMed: 26683026]

Kawano M, Hirano T, Matsuda T, Taga T, Horii Y, Iwato K, Asaoku H, Tang B, Tanabe O, Tanaka H, et al. Autocrine generation and requirement of BSF-2/IL-6 for human multiple myelomas. Nature. 1988; 332:83–85. [PubMed: 3258060]

Küppers R. Mechanisms of B-cell lymphoma pathogenesis. Nat Rev Cancer. 2005; 5:251–262. [PubMed: 15803153]

Lam LT, Wright G, Davis RE, Lenz G, Farinha P, Dang L, Chan JW, Rosenwald A, Gascoyne RD, Staudt LM. Cooperative signaling through the signal transducer and activator of transcription 3 and nuclear factor-kappaB pathways in subtypes of diffuse large B-cell lymphoma. Blood. 2008; 111:3701–3713. [PubMed: 18160665]

Lecault V, Vaninsberghe M, Sekulovic S, Knapp DJ, Wohrer S, Bowden W, Viel F, McLaughlin T, Jarandehei A, Miller M, et al. High-throughput analysis of single hematopoietic stem cell proliferation in microfluidic cell culture arrays. Nat Methods. 2011; 8:581–586. [PubMed: 21602799]

Lee DY, Li YS, Chang SF, Zhou J, Ho HM, Chiu JJ, Chien S. Oscillatory flow-induced proliferation of osteoblast-like cells is mediated by alphavbeta3 and beta1 integrins through synergistic interactions of focal adhesion kinase and Shc with phosphatidylinositol 3-kinase and the Akt/mTOR/p70S6K pathway. J Biol Chem. 2010; 285:30–42. [PubMed: 19889638]

Lenz G, Davis RE, Ngo VN, Lam L, George TC, Wright GW, Dave SS, Zhao H, Xu W, Rosenwald A, et al. Oncogenic CARD11 mutations in human diffuse large B cell lymphoma. Science. 2008a; 319:1676–1679. [PubMed: 18323416]

Lenz G, Wright G, Dave SS, Xiao W, Powell J, Zhao H, Xu W, Tan B, Goldschmidt N, Iqbal J, et al. Lymphoma/Leukemia Molecular Profiling Project. Stromal gene signatures in large-B-cell lymphomas. N Engl J Med. 2008b; 359:2313–2323. [PubMed: 19038878]

Li D, Tang T, Lu J, Dai K. Effects of flow shear stress and mass transport on the construction of a large-scale tissue-engineered bone in a perfusion bioreactor. Tissue Eng Part A. 2009; 15:2773–2783. [PubMed: 19226211]

McLaughlin P, Grillo-López AJ, Link BK, Levy R, Czuczman MS, Williams ME, Heyman MR, Bence-Bruckler I, White CA, Cabanillas F, et al. Rituximab chimeric anti-CD20 monoclonal antibody therapy for relapsed indolent lymphoma: half of patients respond to a four-dose treatment program. J Clin Oncol. 1998; 16:2825–2833. [PubMed: 9704735]

Nakao Y, Kimura H, Sakai Y, Fujii T. Bile canaliculi formation by aligning rat primary hepatocytes in a microfluidic device. Biomicrofluidics. 2011; 5:22212. [PubMed: 21799718]

Ngo VN, Young RM, Schmitz R, Jhavar S, Xiao W, Lim KH, Kohlhammer H, Xu W, Yang Y, Zhao H, et al. Oncogenically active MYD88 mutations in human lymphoma. Nature. 2011; 470:115–119. [PubMed: 21179087]

Nguyen TK, Jordan N, Friedberg J, Fisher RI, Dent P, Grant S. Inhibition of MEK/ERK1/2 sensitizes lymphoma cells to sorafenib-induced apoptosis. Leuk Res. 2010; 34:379–386. [PubMed: 20117835]

Poincloux R, Collin O, Lizárraga F, Romao M, Debray M, Piel M, Chavrier P. Contractility of the cell rear drives invasion of breast tumor cells in 3D Matrigel. Proc Natl Acad Sci USA. 2011; 108:1943–1948. [PubMed: 21245302]

Roschewski M, Staudt LM, Wilson WH. Diffuse large B-cell lymphoma-treatment approaches in the molecular era. Nat Rev Clin Oncol. 2014; 11:12–23. [PubMed: 24217204]

Ruan J, Hajjar K, Rafii S, Leonard JP. Angiogenesis and anti-angiogenic therapy in non-Hodgkin's lymphoma. Ann Oncol. 2009; 20:413–424. [PubMed: 19088170]

Ruan J, Luo M, Wang C, Fan L, Yang SN, Cardenas M, Geng H, Leonard JP, Melnick A, Cerchietti L, Hajjar KA. Imatinib disrupts lymphoma angiogenesis by targeting vascular pericytes. Blood. 2013; 121:5192–5202. [PubMed: 23632889]

Scott DW, Gascoyne RD. The tumour microenvironment in B cell lymphomas. Nat Rev Cancer. 2014; 14:517–534. [PubMed: 25008267]

Singh, A., Brito, I., Lammerding, J. Beyond tissue stiffness and bio-adhesivity: advanced biomaterials to model tumor microenvironments and drug resistance. Trends Cancer. 2018. Published online March 10, 2018. https://doi.org/10.1016/j.trecan.2018.01.008

Spurgeon SE, Coffey G, Fletcher LB, Burke R, Tyner JW, Druker BJ, Betz A, DeGuzman F, Pak Y, Baker D, et al. The selective SYK inhibitor P505-15 (PRT062607) inhibits B cell signaling and function in vitro and in vivo and augments the activity of fludarabine in chronic lymphocytic leukemia. J Pharmacol Exp Ther. 2013; 344:378–387. [PubMed: 23220742]

Tian YF, Ahn H, Schneider RS, Yang SN, Roman-Gonzalez L, Melnick AM, Cerchietti L, Singh A. Integrin-specific hydrogels as adaptable tumor organoids for malignant B and T cells. Biomaterials. 2015; 73:110–119. [PubMed: 26406451]

Tjin EP, Groen RW, Vogelzang I, Derksen PW, Klok MD, Meijer HP, van Eeden S, Pals ST, Spaargaren M. Functional analysis of HGF/MET signaling and aberrant HGF-activator expression in diffuse large B-cell lymphoma. Blood. 2006; 107:760–768. [PubMed: 16189274]

Tzima E, del Pozo MA, Shattil SJ, Chien S, Schwartz MA. Activation of integrins in endothelial cells by fluid shear stress mediates Rho-dependent cytoskeletal alignment. EMBO J. 2001; 20:4639–4647. [PubMed: 11532928]

Wilson WH, Young RM, Schmitz R, Yang Y, Pittaluga S, Wright G, Lih CJ, Williams PM, Shaffer AL, Gerecitano J, et al. Targeting B cell receptor signaling with ibrutinib in diffuse large B cell lymphoma. Nat Med. 2015; 21:922–926. [PubMed: 26193343]

Wojciechowski W, Li H, Marshall S, Dell'Agnola C, Espinoza-Delgado I. Enhanced expression of CD20 in human tumor B cells is controlled through ERK-dependent mechanisms. J Immunol. 2005; 174:7859–7868. [PubMed: 15944291]

Yang Y, Shaffer AL 3rd, Emre NC, Ceribelli M, Zhang M, Wright G, Xiao W, Powell J, Platig J, Kohlhammer H, et al. Exploiting synthetic lethality for the therapy of ABC diffuse large B cell lymphoma. Cancer Cell. 2012; 21:723–737. [PubMed: 22698399]

Yee C, Biondi A, Wang XH, Iscove NN, de Sousa J, Aarden LA, Wong GG, Clark SC, Messner HA, Minden MD. A possible autocrine role for interleukin-6 in two lymphoma cell lines. Blood. 1989; 74:798–804. [PubMed: 2787680]

Yoon SO, Zhang X, Freedman AS, Zahrieh D, Lossos IS, Li L, Choi YS. Down-regulation of CD9 expression and its correlation to tumor progression in B lymphomas. Am J Pathol. 2010; 177:377–386. [PubMed: 20566742]

Yu W, Qu H, Hu G, Zhang Q, Song K, Guan H, Liu T, Qin J. A microfluidic-based multi-shear device for investigating the effects of low fluid-induced stresses on osteoblasts. PLoS One. 2014; 9:e89966. [PubMed: 24587156]

Highlights

- The role of microenvironment-mediated biophysical forces in human lymphomas is unclear
- Fluid flow modulates proliferation and therapeutic response in lymphoma cells
- Fluid flow mechanomodulates B cell receptors and integrins, similar to xenografts
- Fluid flow differentially regulates signaling pathways in subsets of ABC-DLBCLs

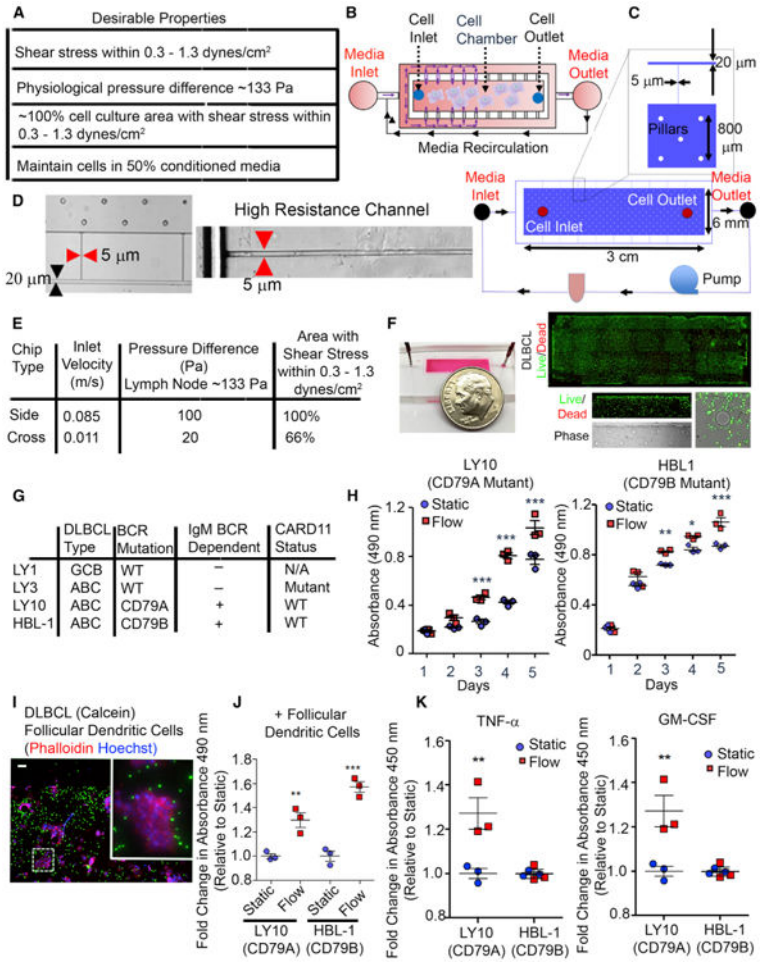

Figure 1. Effect of Fluid Shear Stress on Proliferation and Cytokine Secretion in Human DLBCLs

(A) Table represents desirable properties in a micro-reactor to mimic biophysical conditions in lymphoma microenvironment.

(B) Schematic represents layout of the side-flow micro-reactor. Media enters the outer circulation channels through “Media Inlet” port and perfuses into the central cell culture chamber through high-resistance channel (arrows). Cell suspension is added through “Cell Inlet” port into the middle chamber of the micro-reactor. Black arrowheads represent media recirculation between inlet and outlet ports.

(C) Side-flow micro-reactor with dimensions and relevant design features.

(D) Micrographs of the micro-reactor with 20-µm-wide media flow channel and 5-µm-wide high-resistance channel. The central chamber where cells are cultured is shown to contain equally spaced PDMS pillars.

(E) Table summarizing the COMSOL results.

(F) Left: A photograph of red food dye-loaded side-flow micro-reactor. Right: immunofluorescence image of entire side-flow micro-reactor with calcein (green, live)- and ethidium homodimer I (red, dead)-stained ABC-DLBCL over 48 hr.

(G) Table representing cell lines with DLBCL subtypes and BCR mutation.

(H) Proliferation of HBL-1 and OCI-LY10 cells under static or flow conditions (1.3 dyn/cm^2) maintained over 5 days. Proliferation was quantified with MTS assay, where an increased absorbance corresponds to increased proliferation (mean ±SEM; n=3; *p< 0.05, **p < 0.01, ***p < 0.001 compared to static conditions, two-way ANOVA with Bonferroni's correction).

(I) Immunofluorescence images indicating the distribution of follicular dendritic cells and ABC-DLBCL line HBL-1 inside a side-flow micro-reactor over 48 hr. Scale bar: 20 μm.

(J) Proliferation of HBL-1 and OCI-LY10 cells under static or flow conditions (1.3 dyn/cm^2) maintained over 5 days, in the presence of follicular dendritic cells (mean ± SEM; n = 3; **p < 0.01, ***p < 0.001 compared to static conditions, one-way ANOVA with Tukey's test).

(K) Scatterplots represent ELISA analysis of GM-CSF and TNFα secreted into the culture media by DLBCLs under static and flow conditions (mean ± SEM; n = 3; **p < 0.01 compared to static, two-tailed unpaired t test). Each plot is representative of n = 3 independent repeats. See also Figures S1–S4.

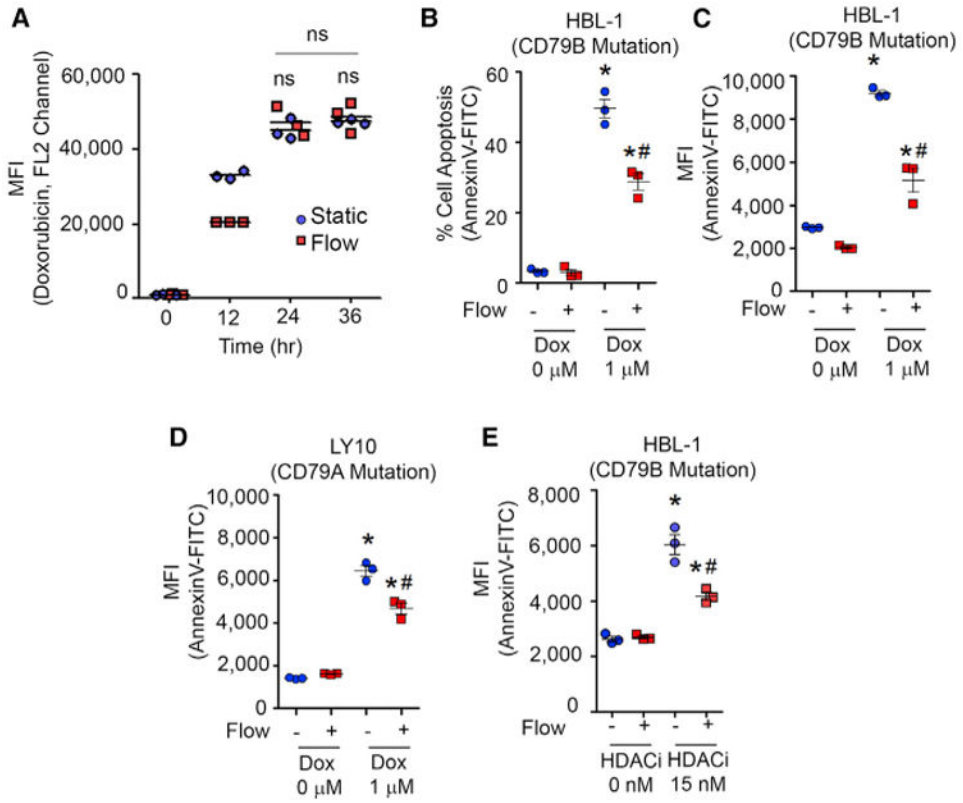

Figure 2. Effect of Fluid Shear Stress on Drug Response in Human DLBCLs

(A) Doxorubicin uptake over 36 hr under static versus flow conditions (1.3 dyn/cm^2) maintained over 3 days (mean ± SEM; n = 3; *p < 0.05 compared to static conditions, two-way ANOVA with Bonferroni's correction). Fluid shear stress was maintained at 1.3 dyn/cm^2 for the entire duration. MFI, mean fluorescence intensity.

(B and C) Scatterplots represent percentage apoptosis (B) and MFI (C) in HBL-1 ABC-DLBCLs exposed to doxorubicin. HBL-1 cells were cultured for 72 hr in micro-reactors and exposed to 1 μM doxorubicin for 24 hr. Fluid shear stress was maintained at 1.3 dyn/cm^2 for the entire 96 hr. HBL-1 cells were stained with fluorescent-tagged anti-IgM antibody and Annexin V-FITC for apoptosis analysis (mean ± SEM; n = 3; *p < 0.05 compared to corresponding 0 μM doxorubicin group, $^{\#}$p < 0.05 compared to static 1 μM group, two-way ANOVA with Bonferroni's correction).

(D) Effect of fluid flow on doxorubicin (1 μM) response in OCI-LY10 ABC-DLBCL, cultured in static versus flow condition. Fluid shear stress was maintained at 1.3 dyn/cm^2 for the entire 96 hr (mean ± SEM; n = 3; *p < 0.05 compared to corresponding 0 μM group, $^{\#}$p < 0.05 compared to static 1 μM group [two-way ANOVA with Bonferroni's correction]).

(E) Scatterplots represent MFI in ABC-DLBCLs exposed to histone deacetylase inhibitor (HDACi) panobinostat. Cells were cultured for 72 hr in micro-reactors and exposed to HDACi for 24 hr. Fluid shear stress was maintained at 1.3 dyn/cm^2 for the entire 96 hr (mean ± SEM; n = 3; *p < 0.05 compared to corresponding 0 μM group, $^{\#}$p < 0.05 compared to static 1 μM group; two-way ANOVA with Bonferroni's correction). Each plot is representative of n = 3 independent repeats.

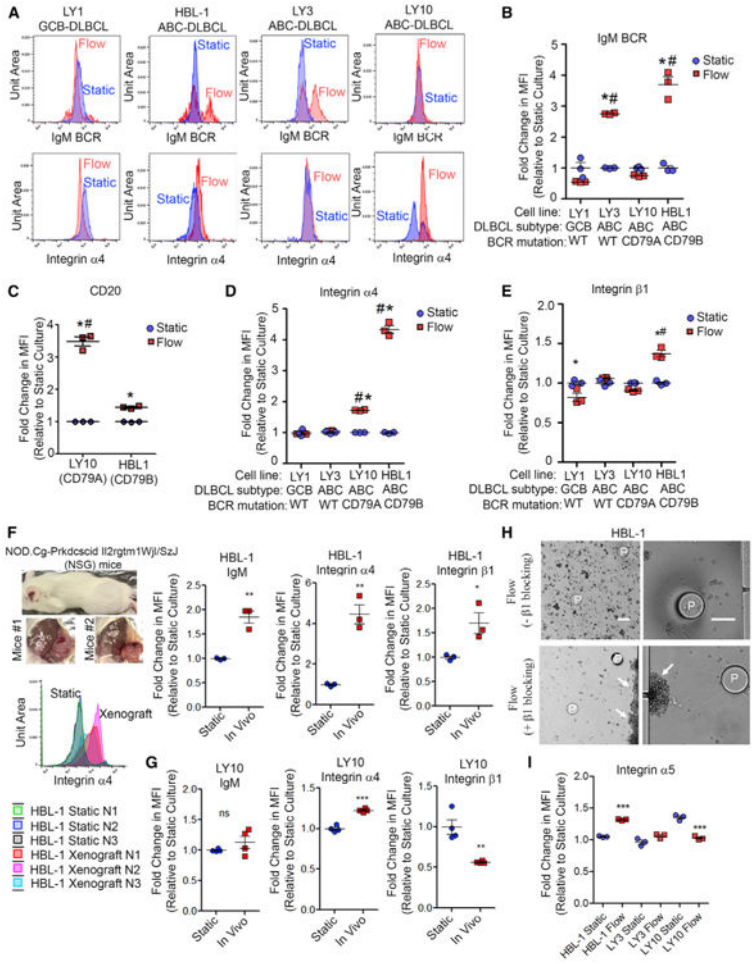

Figure 3. Effect of Fluid Flow on Integrin and B Cell Receptor Expression in Human ABC- and GCB-DLBCLs

(A) Histogram overlays represent flow cytometry analysis of the surface expression level of IgM B cell receptor (BCR) (top) and integrin α4 (bottom) in ABC-DLBCL cell lines OCI-LY3, OCI-LY10, and HBL-1, and GCB-DLBCL cell line OCI-LY1 under static or flow conditions.

(B–E) Scatterplots represent flow cytometry analysis of the surface expression level of IgM BCR (B), CD20 (C), integrin α4(D), and integrin β1 (E) in DLBCLs under static or flow conditions. Fluid shear stress was maintained at 1.3 dyn/cm^2 for the entire 4 days (mean ± SEM; n = 3; *p <0.05 compared to static group, #p < 0.05 compared to the other cell lines, two-way ANOVA with Bonferroni's correction). MFI, mean fluorescence intensity.

(F) Image represents NSG mice implanted with OCI-LY10 xenografts. After 4 weeks of engraftment, tumors were harvested for analysis. Histogram overlays represent flow cytometry analysis of the surface expression level of integrin α4 (bottom). Scatterplots (top right) represent flow cytometry analysis of the surface expression level of IgM BCR, integrin α4, and integrin β1 in static versus in vivo HBL-1 xenografts (mean ± SEM; n = 3; *p < 0.05, **p < 0.005, ***p < 0.001 compared to static group, two-tailed unpaired t test).

(G) Scatterplots represent flow cytometry analysis in static versus in vivo OCI-LY10 xenografts (mean ± SEM; n = 3; *p < 0.05, **p < 0.005, ***p < 0.001 compared to static group, two-tailed unpaired t test).

(H) Micrograph representing 2D culture of ABC-DLBCLs under flow conditions (1.3 dyn/cm^2) with or without integrin β blocking. Letter P represents pillars in the micro-reactor. Images are representative of n = 3 independent repeats. Scale bar: 40 μm.

(I) Scatterplot represents flow cytometry analysis of the surface expression level of integrin α5 in OCI-LY3, HBL-1, and OCI-LY10. Fluid shear stress was maintained at 1.3 dyn/cm^2 for the entire 4 days (mean ± SEM; n = 3; ***p < 0.001 compared to static group, one-way ANOVA with Tukey's test). Each plot is representative of n = 3 independent repeats. See also Figure S5.

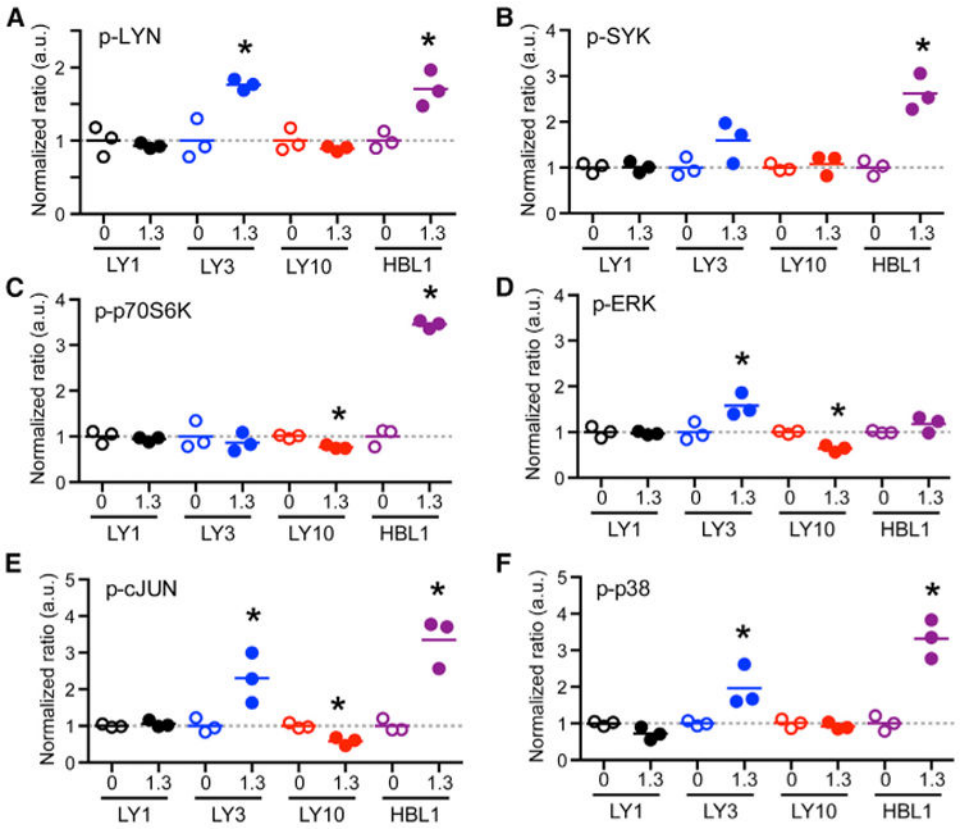

Figure 4. Effect of Fluid Flow on Phosphorylation of Intracellular Signaling Proteins

(A–F) GCB-DLBCL (OCI-LY1) and ABC-DLBCL (OCI-LY3, OCI-LY10, HBL-1) cells were exposed to flow rates inducing 0 or 1.3 dyn/cm^2 shear stress for 72 hr. Levels of the phosphoproteins p-LYN (Tyr^{507}) (A), p-SYK (Tyr^{352}) (B), p-p70 S6K (Thr^{389}/Thr^{412}) (C), p-ERK 1/2 (Thr^{185}/Tyr^{187}) (D), p-cJUN (Ser^{73}) (E), and p-p38 (Thr^{180}/Tyr^{182}) (F) were measured by multiplex Luminex assays. Data were normalized to β-tubulin levels (by sample) and then fold-change normalized to static cultures (by cell line). Dots from n = 3 biological replicates with a line at the mean. *Significant at $p < 0.05$. Fluid shear stress was maintained at 1.3 dyn/cm^2 for the entire 4 days. These experiments were repeated three times.

See also Figure S6.

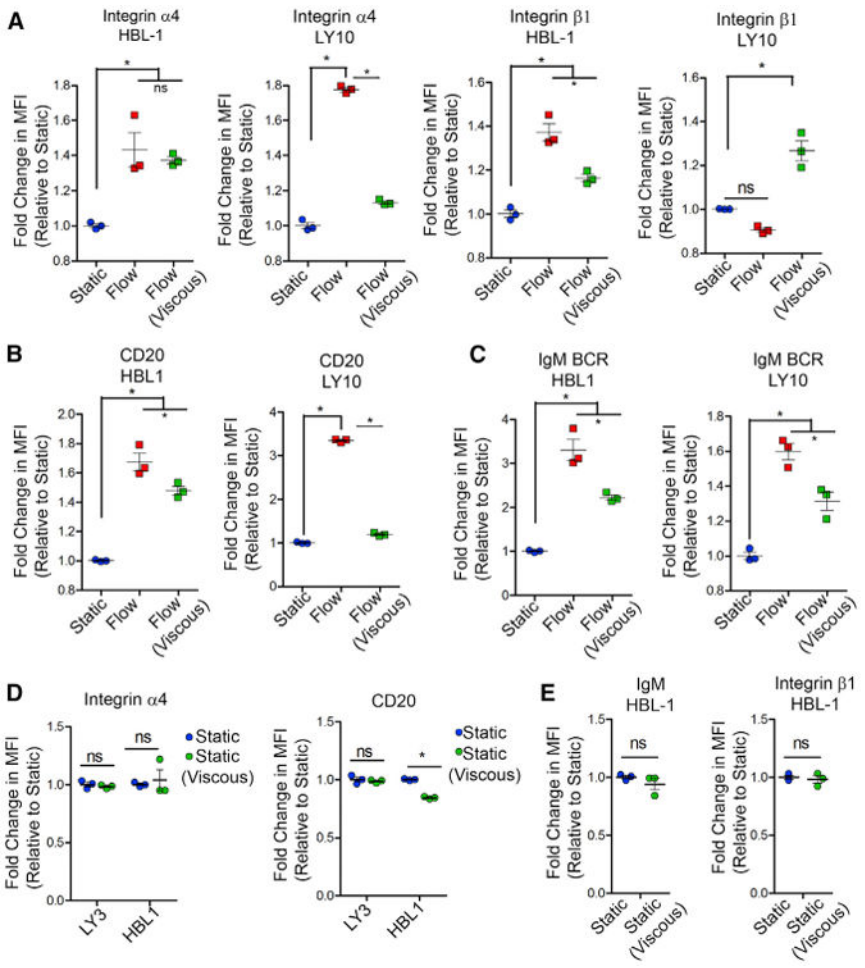

Figure 5. Understanding the Contributions of Fluid Shear Stress and Mass Transport in Mechanomodulation of DLBCLs

(A–C) Fold change in the surface receptor expression of integrin (A), CD20 (B), and IgM BCR (C), using dextran-based viscous media (mean ± SEM; n = 3; *p < 0.05 compared to all groups for A–C, one-way ANOVA with Tukey's test). MFI, mean fluorescence intensity.

(D) Fold change in the surface receptor expression of integrin and CD20 under static versus static (viscous) conditions (mean ± SEM; n = 3; *p < 0.05 compared to static, one-way ANOVA with Tukey'stest).

(E) The effect of static (viscous) condition on surface receptor expression of IgM BCR and β1 integrin in HBL-1 ABC-DLBCL using a dextran-based viscous media (mean ± SEM, n = 3, *p <0.05 compared to static, two-tailed unpaired t test). All results represent 4 days experiments with or without flow. Each plot is representative of n =3 independent repeats. See also Figure S7.

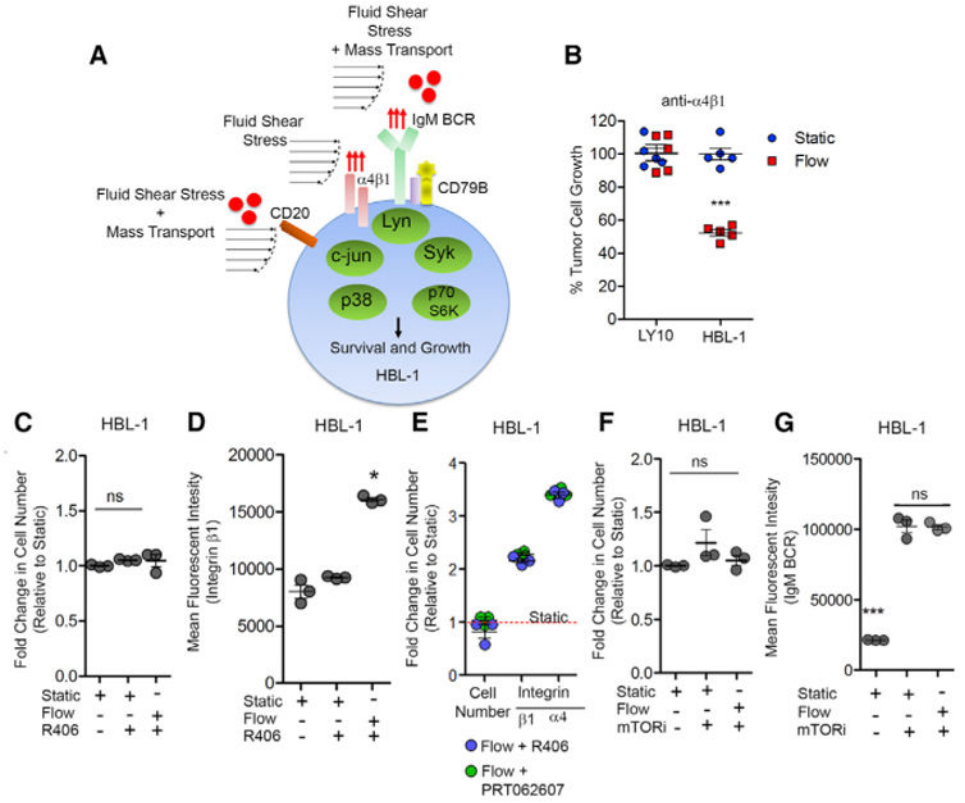

Figure 6. Proposed Mechanistic Model and Effect of Inhibiting Signaling Pathways

(A) Schematic represents the proposed model of fluid shear stress and mass transport-based mechanosignaling of HBL-1 ABC-DLBCL with CD79B mutation. Red arrows represent increased expression level of the specified surface marker. Red circles represent nutrient mass transport.

(B) Dot plots represent growth percentage normalized to static conditions without any blocking antibodies (mean ± SEM; n = 5; *p < 0.05 compared to all groups, two-way ANOVA with Bonferroni's correction). Integrin receptors were blocked with α4β1 antibody over 48 hr with recirculating media in micro-reactors.

(C and D) Effect of SYK inhibition (R406, 200 nM) on (C) HBL-1 cell growth and (D) integrin β1 over 48 hr (mean ± SEM, n =3,*p < 0.05 compared to all groups, one-way ANOVA with Tukey's test).

(E) Comparative effects of two SYK inhibitors (R406, 200 nM; PRT062607; 5 nM) on cell growth over 48 hr (mean ± SEM; n = 3; two-tailed unpaired t test was performed to compare Flow+R406 and Flow+PRT062607).

(F and G) Effect of mTOR inhibition on (F) cell growth and (G) IgM BCR over 48 hr (mean ± SEM; n = 3; *p < 0.05 compared to all groups, one-way ANOVA with Tukey's test). “ns” represent p > 0.05. In all experiments with fluid flow, the fluid shear stress was maintained at 1.3 dyn/cm^2 for the entire duration. Each plot is representative of n = 3 independent repeats. See also Figure S7.

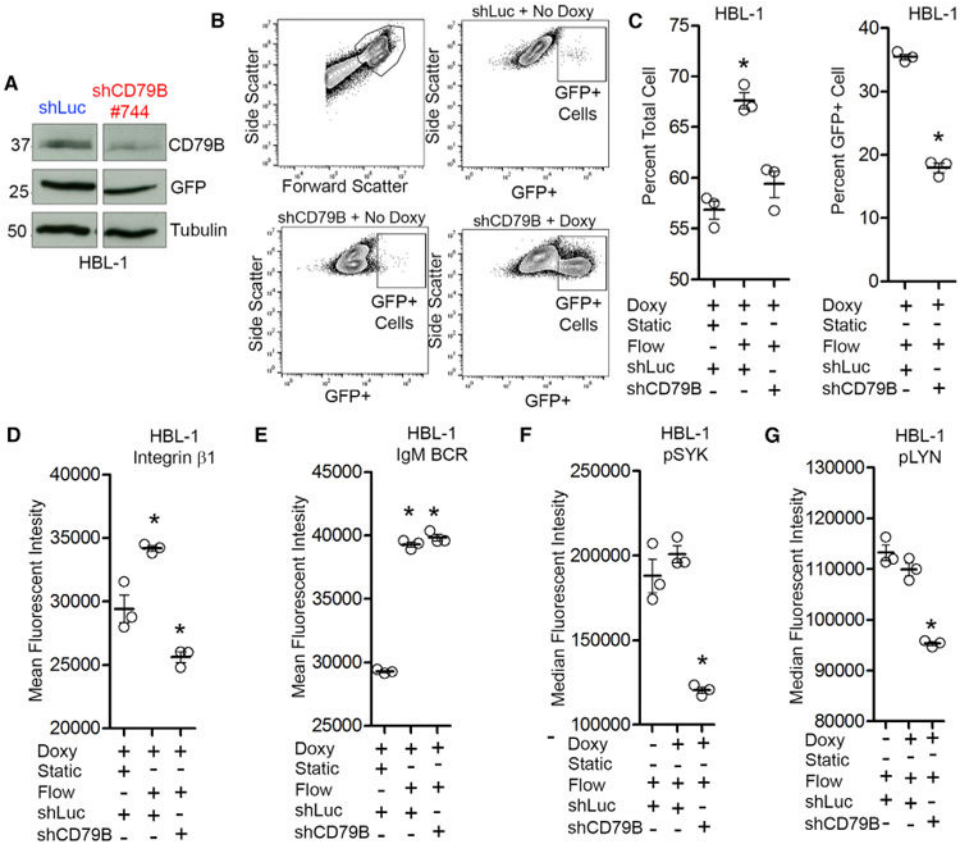

Figure 7. The CD79B Complex Cross Talk with Fluid Flow in Mechanomodulation of DLBCLs

(A) Western blot indicating knockdown of CD79B in HBL-1 using a doxycycline-inducible shRNA against CD79B (shRNA744) or Luciferase (shRNALuc). Induced shRNA encoded expression of GFP in cells. Tubulin served as control.

(B) Scatterplots represents flow cytometry gating and expression of GFP in HBL-1 cells, exposed to doxycycline and fluid flow for 72 hr.

(C) Dot plots represent total cell percentage and GFP^+ cell percentage, each indicating the effect of CD79B knockdown under flow conditions (mean ±SEM; n=3; *$p < 0.05$ compared to all groups).

(D and E) Dot plots represent integrin β1 (D) and IgM (E) expression in GFP^+ cells, indicating the cross talk of CD79B mutation with these surface proteins under fluid flow conditions (mean ± SEM; n = 3; *$p < 0.05$ compared to all groups).

(F and G) Dot plots represent p-SYK (F) and p-LYN (G) expression in GFP^+ cells, suggesting increase in tumor growth under fluid flow conditions is further mediated by downstream p-SYK and p-LYN (mean ± SEM; n = 3; *$p < 0.05$ compared to all groups). In all experiments, a one-way ANOVA with Tukey's test was used for statistical comparison. In all experiments with fluid flow, the fluid shear stress was maintained at 1.3 dyn/cm^2 for the entire duration. These experiments were repeated three times. See also Figure S7.